Hole subbands in strained GaAs-$Ga_{1-x}Al_xAs$ quantum wells: Exact solution of the effective-mass equation

Lucio Claudio Andreani, Alfredo Pasquarello, and Franco Bassani
Scuola Normale Superiore, 56100 Pisa, Italy
(Received 24 February 1987)

Valence subbands of uniaxially stressed GaAs-$Ga_{1-x}Al_xAs$ quantum wells are found by solving exactly the multiband effective-mass equation for the envelope function; as in the particle in a box problem, we first solve the effective-mass equation in each bulk material, and then we impose boundary conditions on the linear combinations of bulk solutions. Discrete symmetries of the effective-mass Hamiltonian are used to decouple the spin-degenerate subbands; the energy levels are obtained as the zeros of an 8×8 determinant. The functional form of the wave functions is given analytically, and is used in order to discuss the heavy-hole–light-hole mixing at finite values of the in-plane vector $\mathbf{k}_\parallel$; the mixing greatly increases when the applied stress reduces the energy separation at $\mathbf{k}_\parallel=0$. Resonances are shown to arise and are due to the degeneracy of discrete levels with states of the continuum at different values of $\mathbf{k}_\parallel$.

I. INTRODUCTION

Semiconductor heterostructures receive great attention today, due to their intrinsic interest and to possible applications in electronic devices. Many methods have been employed to study their electronic structure and optical properties: among these, the envelope-function,[1–5] tight-binding,[6] pseudopotential,[7] and density functional method.[8]

The envelope-function approach, based on the effective-mass approximation, is easy to apply; it gives a reasonable description of conduction and valence subbands near the center of the Brillouin zone, provided the constituent materials are chemically similar, like in the GaAs-$G_{1-x}Al_xAs$ system. In addition, it is particularly suited to include external perturbations, like uniaxial stress[9] and magnetic field.[3] Perhaps the most important prediction of the effective mass theory is the mixing of heavy and light holes away from $\mathbf{k}_\parallel=0$; this mixing gives rise to conspicuous nonparabolicities in the space-quantized valence-band structure, and it has a great effect on all optical properties of heterostructures, like resonant Raman scattering,[10] polarization of the luminescence,[11] and exciton binding energy.[12] When the Γ_8 valence band is described by the 4×4 Luttinger kinetic matrix, the mixing arises from off-diagonal terms and from current conserving boundary conditions at the interface. Even if in some cases the observed mixing is too large to be accounted for by the simple effective mass theory,[11] this approach remains nonetheless a very useful tool in order to understand the optical properties of superlattices near the band edge.

In this paper we adopt the four-component envelope-function formalism in order to study the valence subbands of an isolated quantum well under compressive stress in the growth direction; we show that the effective-mass equation can be solved exactly, and compare our results with those of the variational treatments employed so far. The method of solution is an extension of the particle in a box problem of quantum mechanics: we first solve the effective-mass equation in the well and barrier materials, and then match the linear combinations of bulk wave functions at the interfaces in order to find the eigenstates. The components of the envelope function turn out to be trigonometric functions inside the well and decreasing exponentials outside (possibly of complex argument), even at nonzero in-plane wave vector.

Our method, while in principle equivalent to the variational solution of previous authors, has several distinct features. First, off-diagonal terms of the Luttinger Hamiltonian, current conserving boundary conditions, and warping of the subbands in the k_xk_y plane are taken into account exactly. Second, the wave functions are given analytically and are found to be simple; the envelope function is determined with the same accuracy in all regions of space, even in the barriers, when the components are small and the variational method is less accurate; this may be useful in the study of tunneling phenomena. Third, resonant levels above the well, degenerate with the continuum, are naturally found with this approach. On the other hand, it must be remarked that our calculation is not self-consistent, and it applies as it stands only to undoped materials.

The remaining part of the paper is organized as follows. In Sec. II we discuss the solutions of the effective-mass equation in each bulk semiconductor, and we show how the boundary conditions give rise to discrete levels. In Sec. III we study discrete symmetries acting on the four-component envelope function, and we use the transformation properties of the envelope function under specular reflection to decouple the spin degenerate subbands. In Sec. IV we present the results, and treat a number of topics: heavy-hole–light-hole (HH–LH) mixing, the effect of stress, and Fano resonances. We also compare our wave functions with the variational results

of Altarelli. In Sec. V we summarize results and conclusions.

II. EXACT SOLUTION OF THE EFFECTIVE-MASS EQUATION

We consider an isolated quantum well grown in a $\langle 100 \rangle$ direction, which we take along the quantization axis z. The well extends from $-L/2$ to $L/2$. The effective mass Hamiltonian describing the Γ_8 valence band is a 4×4 matrix operator quadratic in $\mathbf{k}=-i\nabla$, given by[13]

$$H=-\begin{bmatrix} P+Q & L & M & 0 \\ L^\dagger & P-Q & 0 & M \\ M^\dagger & 0 & P-Q & -L \\ 0 & M^\dagger & -L^\dagger & P+Q \end{bmatrix}+V(z) , \tag{1}$$

where

$$\begin{aligned} P&=\frac{\gamma_1}{2m_0}k^2 , \\ Q&=\frac{\gamma_2}{2m_0}(k_x^2+k_y^2-2k_z^2) , \\ L&=\frac{-i\sqrt{3}\gamma_3}{m_0}(k_x-ik_y)k_z , \\ M&=\frac{\gamma_2\sqrt{3}}{2m_0}(k_x^2-k_y^2)-i\frac{\gamma_3\sqrt{3}}{m_0}k_xk_y , \end{aligned} \tag{2}$$

and $V(z)$ is a square-well potential which vanishes inside the well and equals $-V_0$ in the barriers. The Luttinger parameters $\gamma_1,\gamma_2,\gamma_3$ are those appropriate to the well or barrier materials. The Hamiltonian (1) acts on a four-component envelope function $\underline{F}=(F_1,F_2,F_3,F_4)$, and the electronic wave functions are approximately given by

$$\begin{aligned} \Psi(\mathbf{r})=&F_1(\mathbf{r})\,|\,\tfrac{3}{2}\tfrac{3}{2}\rangle+F_2(\mathbf{r})\,|\,\tfrac{3}{2}\tfrac{1}{2}\rangle+F_3(\mathbf{r})\,|\,\tfrac{3}{2}-\tfrac{1}{2}\rangle \\ &+F_4(\mathbf{r})\,|\,\tfrac{3}{2}-\tfrac{3}{2}\rangle . \end{aligned} \tag{3}$$

The Γ_8 Bloch functions of both materials at $\mathbf{k}=\mathbf{0}$ can be expressed in terms of the space Bloch functions X, Y, and Z, and of the spin functions α and β

$$\begin{aligned} |\,\tfrac{3}{2}\tfrac{3}{2}\rangle&=\frac{1}{\sqrt{2}}(X+iY)\alpha , \\ |\,\tfrac{3}{2}\tfrac{1}{2}\rangle&=\frac{i}{\sqrt{6}}[(X+iY)\beta-2Z\alpha] , \\ |\,\tfrac{3}{2}-\tfrac{1}{2}\rangle&=\frac{1}{\sqrt{6}}[(X-iY)\alpha+2Z\beta] , \\ |\,\tfrac{3}{2}-\tfrac{3}{2}\rangle&=\frac{i}{\sqrt{2}}(X-iY)\beta . \end{aligned} \tag{4}$$

X, Y, and Z being the partner functions of the representation Γ_{15} of the zinc-blende point group T_d, which transform as the $\mathbf{p}$ functions on the two sublattices.

The effect of a uniaxial stress along [001] is to add to (1) a strain Hamiltonian,[14,15]

$$H_\zeta=\begin{bmatrix} -\zeta & 0 & 0 & 0 \\ 0 & \zeta & 0 & 0 \\ 0 & 0 & \zeta & 0 \\ 0 & 0 & 0 & -\zeta \end{bmatrix} , \tag{5}$$

with

$$\zeta=b(S_{11}-S_{12})X , \tag{6}$$

where b is a deformation potential, S_{11} and S_{12} are the compliance constants, and X is the applied stress. Hence, the effect of stress along [001] is to modify the Q term of (2) to

$$Q=\frac{\gamma_2}{2m_0}(k_x^2+k_y^2-2k_z^2)+\zeta . \tag{7}$$

We first discuss the solutions of the wave equation in the bulk. The components of the Bloch vector $\mathbf{k}$ are good quantum numbers, and the envelope function can be taken of the form $\underline{F}(\mathbf{r})=\underline{f}e^{i\mathbf{k}\cdot\mathbf{r}}$, where $\underline{f}=(f_1,f_2,f_3,f_4)$ is an eigenvector of the Luttinger kinetic matrix, and k_x,k_y,k_z are real numbers. The secular equation gives the well-known hole dispersion relation

$$E=-P\pm(Q^2+LL^\dagger+MM^\dagger)^{1/2} . \tag{8}$$

The plus sign refers to heavy holes, the minus sign to light holes. Each eigenvalue is twofold degenerate, since the Hamiltonian is both inversion and time-reversal invariant.

The explicit form of the eigenvectors is easily obtained, and is given below for later use:

$$\begin{aligned} L_1(\mathbf{k})&=\begin{bmatrix} R_1 \\ L^\dagger \\ M^\dagger \\ 0 \end{bmatrix}e^{i\mathbf{k}\cdot\mathbf{r}}, \quad L_2(\mathbf{k})=\begin{bmatrix} 0 \\ M \\ -L \\ R_1 \end{bmatrix}e^{i\mathbf{k}\cdot\mathbf{r}} , \\ H_1(\mathbf{k})&=\begin{bmatrix} -L \\ R_2 \\ 0 \\ -M^\dagger \end{bmatrix}e^{i\mathbf{k}\cdot\mathbf{r}}, \quad H_2(\mathbf{k})=\begin{bmatrix} -M \\ 0 \\ R_2 \\ L^\dagger \end{bmatrix}e^{i\mathbf{k}\cdot\mathbf{r}} , \end{aligned} \tag{9}$$

where R_1 and R_2 are defined by

$$R_1=Q-P-E, \quad R_2=Q+P+E . \tag{10}$$

We remark that only two of the eigenvectors (9) are linearly independent.

In the case of the quantum well, the potential $V(z)$ breaks translation symmetry along z; however, k_x and k_y remain good quantum numbers and we can set $\underline{F}(x,y,z)=e^{i(k_xx+k_yy)}\underline{f}(z)$. The effective-mass equation $H\underline{F}=E\underline{F}$ must be supplemented by boundary conditions at each interface. In the approximation that the Bloch functions (4) are equal in the two materials, boundary conditions can be expressed in terms of the envelope functions alone. They require the continuity of each component $f_i(z)$ of the envelope function and of the following vector:[16]

$$\begin{bmatrix} (\gamma_1-2\gamma_2)\frac{\partial}{\partial z} & \sqrt{3}\gamma_3(k_x-ik_y) & 0 & 0 \\ -\sqrt{3}\gamma_3(k_x+ik_y) & (\gamma_1+2\gamma_2)\frac{\partial}{\partial z} & 0 & 0 \\ 0 & 0 & (\gamma_1+2\gamma_2)\frac{\partial}{\partial z} & -\sqrt{3}\gamma_3(k_x-ik_y) \\ 0 & 0 & \sqrt{3}\gamma_3(k_x+ik_y) & (\gamma_1-2\gamma_2)\frac{\partial}{\partial z} \end{bmatrix} \begin{bmatrix} f_1(z) \\ f_2(z) \\ f_3(z) \\ f_4(z) \end{bmatrix} . \tag{11}$$

The continuity of vector (11) generalizes the usual derivative boundary condition, and is equivalent to the Hermiticity of the effective-mass Hamiltonian; it implies the conservation of current through the boundary, provided the Bloch functions at both sides are taken to be equal. This assumption restricts the range of validity of the envelope-function approach to cases in which well and barrier materials have similar chemical properties, like the GaAs-$Ga_xAl_{1-x}As$ quantum well.

To calculate the energy levels corresponding to a given $\mathbf{k}_\parallel$, we use the fact that the potential is a constant in each of the three regions. For each E, we find the eigenfunctions of the Luttinger Hamiltonian with a given $\mathbf{k}_\parallel$, and with the corresponding values of k_z. They are denoted by $\pm k_l$, $\pm k_h$ within the well (Fig. 1), and by $\pm i\chi_l$, $\pm i\chi_h$ in the barrier, where E is replaced by $E-V_0$. Then, we take the most general linear combination of bulk solutions, and we impose boundary conditions at the two interfaces. In order to have confined states, both numbers χ_l, χ_h must have a real part, otherwise we have a continuous spectrum.

Let us count the number of free parameters and of boundary conditions. Inside the well we have eight independent eigenfunctions with given E, $\mathbf{k}_\parallel$; at both sides in the barriers we have only four because of the condition of vanishing at infinity. This makes a total of 16 unknown coefficients. Continuity and current conserving boundary conditions, at both interfaces, are again 16. Hence, we end up with a compatibility condition of the form $D(E,\mathbf{k}_\parallel)=0$, where D is a 16×16 determinant, which gives the subband dispersion in an implicit form.

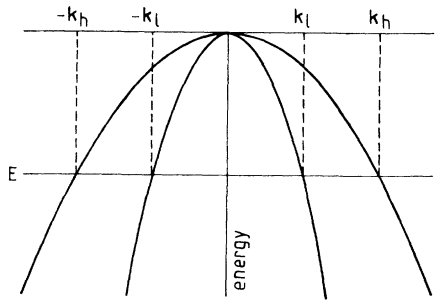

FIG. 1. Schematic representation of the solutions of the heavy- and light-hole dispersion relation at $\mathbf{k}_\parallel=0$ and at fixed E.

The procedure described above can be simplified by using the reflection symmetry σ with respect to the plane $z=0$ and time-reversal symmetry. We will show in Sec. III that the 16×16 determinant decouples in two 8×8 determinants, which yield the Kramers degenerate hole subbands at a given $\mathbf{k}_\parallel$.

III. DISCRETE SYMMETRIES OF THE EFFECTIVE-MASS HAMILTONIAN

A symmetry operator O acts on the electronic wave function Ψ in the following way:

$$O\Psi=F'_1\,|\,\tfrac{3}{2}\tfrac{3}{2}\rangle+F'_2\,|\,\tfrac{3}{2}\tfrac{1}{2}\rangle+F'_3\,|\,\tfrac{3}{2}-\tfrac{1}{2}\rangle+F'_4\,|\,\tfrac{3}{2}-\tfrac{3}{2}\rangle . \tag{12}$$

Consider the time-reversal operator. The Bloch functions X, Y, Z of (4) are invariant under T, while α, β are transformed into one another by $i\sigma_y$. This gives for the envelope function

$$T\begin{bmatrix} F_1(x,y,z) \\ F_2(x,y,z) \\ F_3(x,y,z) \\ F_4(x,y,z) \end{bmatrix} = \begin{bmatrix} 0 & 0 & 0 & -i \\ 0 & 0 & i & 0 \\ 0 & -i & 0 & 0 \\ i & 0 & 0 & 0 \end{bmatrix} \begin{bmatrix} F_1^*(x,y,z) \\ F_2^*(x,y,z) \\ F_3^*(x,y,z) \\ F_4^*(x,y,z) \end{bmatrix} . \tag{13}$$

It can be easily verified that T is a symmetry of the effective-mass Hamiltonian, i.e., $THT^{-1}=H$; moreover, this property is independent on the phase of T.

Though specular reflection with respect to the xy plane is not a symmetry operation of the T_d point group, it is a good symmetry operation for the quantum well problem in the effective-mass approximation because we have neglected k-linear terms in (1). In order to derive its explicit form we express it as $\sigma=R_\pi I$, where $R_\pi=\exp(-i\pi J_z)$, and we obtain

$$\sigma\begin{bmatrix} F_1(x,y,z) \\ F_2(x,y,z) \\ F_3(x,y,z) \\ F_4(x,y,z) \end{bmatrix} = \begin{bmatrix} -1 & 0 & 0 & 0 \\ 0 & 1 & 0 & 0 \\ 0 & 0 & -1 & 0 \\ 0 & 0 & 0 & 1 \end{bmatrix} \begin{bmatrix} F_1(x,y,-z) \\ F_2(x,y,-z) \\ F_3(x,y,-z) \\ F_4(x,y,-z) \end{bmatrix} , \tag{14}$$

apart from an overall phase. We shall denote the eigenvalue of σ by *parity*, not to be confused with the eigen-

value under space inversion I; the reason we are interested in σ is that it leaves the in-plane vector $\mathbf{k}_\parallel$ invariant, whereas I changes the sign of $\mathbf{k}_\parallel$.

By looking at the explicit form of T and σ, it can be seen that the two operators anticommute:

$$\{\sigma, T\}=0 \ . \tag{15}$$

From this important property it follows that T changes the parity eigenvalue of a state. As a consequence we can prove that a symmetry operator exists which changes the function of a given $\mathbf{k}_\parallel$ with a definite parity into a function of the same $\mathbf{k}_\parallel$ with opposite parity. Such a symmetry operator is $R_\pi T$, and its very existence proves that all the bands, double degenerate at every value of $\mathbf{k}_\parallel$, can be chosen with given parity under σ.[17] If one solution is found, the other at the same $\mathbf{k}_\parallel$ is given by

$$R_\pi T F = e^{i\mathbf{k}_\parallel\cdot\mathbf{r}_\parallel}(f_4^*(z), f_3^*(z), f_2^*(z), f_1^*(z)) \ . \tag{16}$$

It can be checked that all boundary conditions are invariant under σ, in the sense that if a wave function of definite parity satisfies boundary conditions at the interface $z=L/2$, it satisfies them at $z=-L/2$ too. Hence, in order to simplify the quantum well problem, it suffices to work with even (or odd) solutions in the two materials, and to impose continuity and current conserving boundary conditions at one interface.

The solutions of definite parity in the two media can be taken as linear combinations of (9) with both signs of k_z. We take L_2, H_2 as independent eigenfunctions, and we choose to work with odd wave functions only.

The envelope function inside the quantum well at given E, $\mathbf{k}_\parallel$ is then

$$\begin{aligned}\underline{f}(z)=&B_1\begin{bmatrix}0\\ M\sin(k_l z)\\ iL_l\cos(k_l z)\\ R_{1l}\sin(k_l z)\end{bmatrix}+B_2\begin{bmatrix}0\\ M\sin(k_h z)\\ iL_h\cos(k_h z)\\ R_{1h}\sin(k_h z)\end{bmatrix}\\ &+B_3\begin{bmatrix}M\cos(k_h z)\\ 0\\ -R_{2h}\cos(k_h z)\\ -iL_h^\dagger\sin(k_h z)\end{bmatrix}+B_4\begin{bmatrix}M\cos(k_l z)\\ 0\\ -R_{2l}\cos(k_l z)\\ -iL_l^\dagger\sin(k_l z)\end{bmatrix},\end{aligned} \tag{17}$$

where k_l, k_h are the roots of the dispersion relation (8), and we have defined $L_l \equiv L(\mathbf{k}_\parallel, k_l)$ and similarly for L_h, R_{1l}, R_{1h}, R_{2l}, R_{2h}. We remark that k_l, k_h need not be necessarily real, since the wave function (17) is defined only for $-L/2<z<L/2$. Note that the second and the fourth component of $\underline{f}$ change sign as $z\to -z$, but the first and the third do not;[18] the overall parity of the envelope function is not related to the position of the nodes.

In the barrier we replace E by $E-V_0$ and we use $\chi_z \equiv -ik_z$ instead of k_z. By keeping only those functions which vanish at infinity, we have, for $z>L/2$,

$$\begin{aligned}\underline{f}(z)=&B_5\begin{bmatrix}0\\ \bar{M}\\ -\bar{L}_l\\ \bar{R}_{1l}\end{bmatrix}e^{-\chi_l z}+B_6\begin{bmatrix}0\\ \bar{M}\\ -\bar{L}_h\\ \bar{R}_{1h}\end{bmatrix}e^{-\chi_h z}\\ &+B_7\begin{bmatrix}-\bar{M}\\ 0\\ \bar{R}_{2h}\\ \bar{L}_h^\dagger\end{bmatrix}e^{-\chi_h z}+B_8\begin{bmatrix}-\bar{M}\\ 0\\ \bar{R}_{2l}\\ \bar{L}_l^\dagger\end{bmatrix}e^{-\chi_l z},\end{aligned} \tag{18}$$

where the overbar indicates that the values of the Luttinger parameters are those appropriate to $Ga_{1-x}Al_xAs$. The envelope function for $z<L/2$ is easily obtained from (18) by applying the reflection operator σ. The condition of vanishing at infinity implies that both χ_l and χ_h must have a nonzero real part, but they may well have an imaginary part (in which case, it is easy to see that $\chi_l=\chi_h^*$); when this happens, the envelope function oscillates at rate $\mathrm{Im}(\chi_l)$, while being damped at a rate $\mathrm{Re}(\chi_l)$. In the continuum χ_l and χ_h have vanishing real part and the expansion (18) must include all oscillating functions.

Attention must be paid to a correct definition of $L^\dagger$ and $\bar{L}^\dagger$. The meaning of $L^\dagger$ is the "Hermitian conjugate of the operator L"; therefore, since $k_z=-i\partial/\partial z$ is an Hermitian operator, k_l and k_h are unchanged under Hermitian conjugation, even if they are imaginary. Similarly, since $\chi_z=-ik_z$ by definition, χ_l and χ_h change sign under Hermitian conjugation.

By imposing boundary conditions at $z=L/2$, we obtain a linear homogeneous system for the coefficients $B_1,\ldots,B_8$. The zeros of the 8×8 determinant of this linear system give the energy eigenvalues of the subbands, for a given $\mathbf{k}_\parallel$ and for each value of the stress parameter ζ.

The determinant depends on the values of the wave functions (17), (18), and of their derivatives at $z=L/2$, given in (11); note that boundary conditions mix different components of the envelope function. We do not give an explicit expression of the determinant because it is rather cumbersome; however, it is easy to obtain it using the above prescription. It has not been possible to evaluate the determinant in a simple form, except in the approximation of infinite well depth, where the 4×4 determinant arising from boundary conditions $\underline{f}=\underline{0}$ gives back the Nedorezov result.[19]

In finding the zeros of the determinant, care must be taken in eliminating spurious solutions, which arise when the bulk wave functions are not linearly independent. This happens in two cases: (a) when $k_l=0$ (or $k_h,\chi_l,\chi_h=0$), (b) when $k_l=k_h$ (or $\chi_l=\chi_h$).

IV. RESULTS FOR HOLE SUBBANDS AND EIGENFUNCTIONS

In this section we present some results referring to a GaAs-$Ga_{1-x}Al_xAs$ quantum well with an aluminum mole fraction $x=0.21$. We use the following values for the Luttinger parameters:[20] $\gamma_1=6.85$, $\gamma_2=2.1$, $\gamma_3=2.9$ for GaAs and $\gamma_1=3.45$, $\gamma_2=0.68$, $\gamma_3=1.29$ for AlAs.

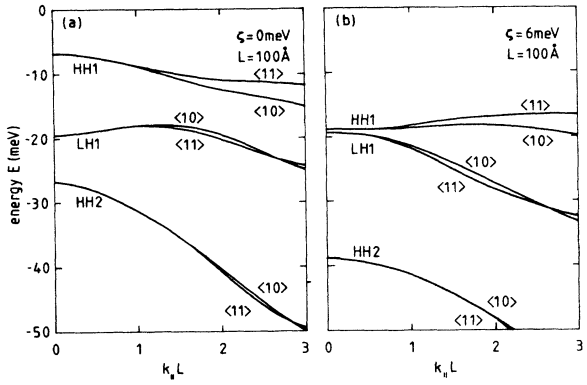

FIG. 2. Dispersion of the three highest valence subbands in a GaAs-$Ga_{0.79}Al_{0.21}As$ quantum well of width $L=100$ Å, (a) with no stress ($\zeta=0$) and (b) with an applied stress $X=2.3$ kbar ($\zeta=6$ meV). In (b) the zero of the energy has been taken to coincide with the top of the bulk GaAs valence band under the same stress.

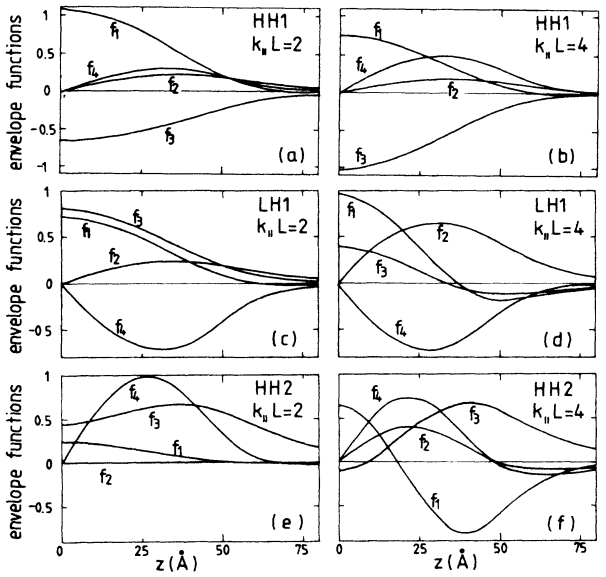

FIG. 3. Envelope-function components of the three highest subbands in the ⟨10⟩ direction in a 100-Å GaAs-$Ga_{0.79}Al_{0.21}As$ quantum well without stress. The wave functions have been calculated for $k_\parallel L=2$ and $k_\parallel L=4$.

The parameters $\gamma_1,\gamma_2,\gamma_3$ for $Ga_{0.79}Al_{0.21}As$ are obtained by linear interpolation. The band gap difference in eV is taken to be[21] $\Delta E_g=1.04x+0.47x^2$. We assume a 40% prescription for the hole barrier depth,[22] which gives a value of $V_0=95.65$ meV. We take[23] $b=-1.7$ eV and $S_{11}=1.17\times10^{-3}$ kbar^{-1}, $S_{12}=-0.37\times10^{-3}$ kbar^{-1}.

In Fig. 2 we show the three highest subbands of a 100-Å-wide quantum well in the two directions ⟨10⟩ and ⟨11⟩; the subbands are calculated for the case of no stress ($\zeta=0$) and for a value $\zeta=6$ meV of the stress parameter, which corresponds to a compressive stress of 2.3 kbar. In Fig. 2(b) the zero of the energy has been taken to coincide with the top of the bulk GaAs valence band under the same stress (we remind that in bulk GaAs the degeneracy between HH and LH at $\mathbf{k}=\mathbf{0}$ is lifted by the application of a uniaxial stress and the LH value is shifted upwards by ζ). The subbands of Fig. 2(a) are highly nonparabolic, due to the mutual repulsion at $\mathbf{k}_\parallel\neq\mathbf{0}$; in particular, LH1 has an electronlike effective mass. A slight warping in the k_xk_y plane is also present. When a uniaxial compressive stress is applied [Fig. 2(b)], the heavy-hole subbands at $\mathbf{k}_\parallel=\mathbf{0}$ are shifted downwards relative to the light holes by an amount 2ζ; the anticrossing behavior arises from the increased repulsion between HH1 and LH1.

In the case of zero stress, we have compared our results with those obtained by Altarelli with a variational procedure.[24] The agreement is found to be excellent for all bound energy states. Sanders and Chang applied the variational method to include a uniaxial stress.[9] Also, in this case we expect good agreement between the two re-

TABLE I. The variational envelope functions obtained by Altarelli are compared with the exact results presented in this paper. The values refer to the highest valence subband (HH1) at $k_\parallel L=4$ in the ⟨10⟩ direction in a 100 Å GaAs-$Ga_{0.79}Al_{0.21}As$ quantum well without stress. The origin of the z axis is at the center of the quantum well.

z (Å)	f_1	f_2	f_3	f_4
		Exact envelope functions		
0	7.481×10^{-2}	0	-1.016×10^{-1}	0
25	5.085×10^{-2}	1.634×10^{-2}	-7.229×10^{-2}	4.745×10^{-2}
50	7.697×10^{-3}	1.405×10^{-2}	-2.005×10^{-2}	3.077×10^{-2}
75	-1.533×10^{-3}	3.614×10^{-3}	-1.948×10^{-3}	3.797×10^{-3}
100	-6.114×10^{-4}	6.768×10^{-4}	-6.837×10^{-5}	3.306×10^{-4}
		Variational envelope functions		
0	7.480×10^{-2}	1.364×10^{-6}	-1.017×10^{-1}	-7.386×10^{-7}
25	5.082×10^{-2}	1.637×10^{-2}	-7.230×10^{-2}	4.742×10^{-2}
50	7.824×10^{-3}	1.397×10^{-2}	-2.000×10^{-2}	3.066×10^{-2}
75	-1.495×10^{-3}	3.570×10^{-3}	-1.976×10^{-3}	3.815×10^{-3}
100	-7.297×10^{-4}	6.996×10^{-4}	1.578×10^{-5}	1.944×10^{-4}

sults, though we have not made a detailed comparison.

In Fig. 3 we give the components of the envelope functions $f(z)$ for HH1, LH1, HH2 in the $\langle 10 \rangle$ direction for the case of no stress; the corresponding subbands are those of Fig. 2(a). We remind that the well extends from -50 to 50 Å. A slight discontinuity in the derivative at $z=50$ Å is present, due to current conserving boundary conditions. It can be seen that LH1 has a higher penetration in the barrier than HH1. We notice that at $k_{\parallel}L=2$ the largest component in HH1 is f_1, whereas the largest component in LH1 is f_3; however, as the wave vector increases to $k_{\parallel}L=4$, the f_3 component of HH1 increases at the expense of f_1, showing that HH1 has more light-hole character. The opposite trend is seen in LH1.

The wave functions shown in Fig. 3 have been compared with variational results obtained with the same set of parameters.[24] This is shown in Table I, where the values of the envelope functions obtained from the variational approach are also given for comparison. A linear combination of the spin-degenerate envelope functions of Altarelli has been taken in order to compare them with our envelope functions, which we have chosen to be odd under the symmetry operator σ. The envelope functions are normalized according to $\int \sum_i |f_i(z)|^2 dz=1$, and z is measured in angstroms. The agreement is excellent inside the well, where the amplitude of the confined level is large; the variational wave function and our exact solution coincide up to one part in a thousand. However, the absolute precision of the variational calculation remains constant in space, and the variational result may considerably differ in the barrier, where the value of the envelope function is greatly reduced. This indicates that differences between variational and exact calculations may show up in the tunneling between two distant quantum wells.

The wave functions for $k_{\parallel}L=4$ of Fig. 3 have values of χ_l, χ_h which have an imaginary part, and which are the complex conjugate of each other. However, since $\mathrm{Re}(\chi_h) > \mathrm{Im}(\chi_h)$, the oscillations implied by (18) are strongly damped and do not seem to be practically observable.

It is clear that HH1 and LH1 are strongly mixed at finite wave vector when their energy separation at $\mathbf{k}_{\parallel}=\mathbf{0}$ is small, as in Fig. 2(b). We now want to give a quantitative measure of this mixing. The components of the envelope function inside the well, according to (17), can be written in the form

$$\underline{f}(z)=\begin{bmatrix} h_1\cos(k_h z)+l_1\cos(k_l z) \\ h_2\sin(k_h z)+l_2\sin(k_l z) \\ h_3\cos(k_h z)+l_3\cos(k_l z) \\ h_4\sin(k_h z)+l_4\sin(k_l z) \end{bmatrix} . \tag{19}$$

At $\mathbf{k}_{\parallel}=\mathbf{0}$ only the first component of HH1 and the third component of LH1 are nonvanishing. To give an estimate of the mixing between the bands, which is produced as we increase the value of $\mathbf{k}_{\parallel}$, we consider the ratio h_3/h_1 for HH1. This ratio equals zero at $\mathbf{k}_{\parallel}=\mathbf{0}$, and it grows as HH1 and LH1 are mixed. Moreover, the overlap integrals with the states of the first conduction band are roughly proportional to h_1 and h_3, so that h_3/h_1 can be related to the ratio I_z/I_x of the two linear polarization components of the luminescence.[11]

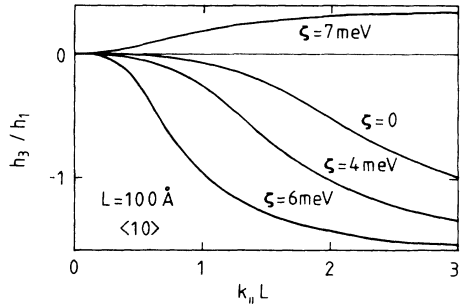

FIG. 4. Ratio h_3/h_1 for the HH1 subband of a 100-Å GaAs-$Ga_{0.79}Al_{0.21}As$ quantum well in the $\langle 10 \rangle$ direction, for the values $\zeta=0,4,6,7$ meV of the stress parameter.

In Fig. 4 we plot the ratio h_3/h_1 as a function of $k_{\parallel}$ in the direction $\langle 10 \rangle$, for the values $\zeta=0,4,6,7$ meV of the stress parameter. As HH1 remains above LH1, the ratio h_3/h_1 at finite wave vector grows rapidly with the applied stress; however, when LH1 becomes higher in energy ($\zeta=7$ meV, not shown in Fig. 2) the HH1 band is pushed downwards and the mixing decreases. This behavior could be observed experimentally by modulating the applied stress and by monitoring the ratio I_z/I_x of the luminescence from the first conduction band; a great enhancement of I_z/I_x is predicted for the value of the

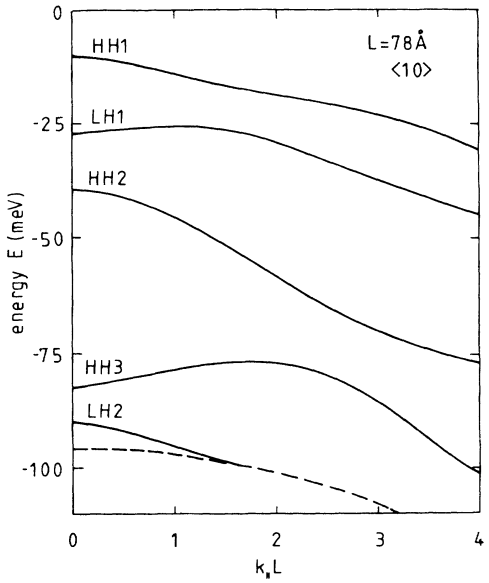

FIG. 5. Confined hole levels in the $\langle 10 \rangle$ direction for a 78-Å GaAs-$Ga_{0.79}Al_{0.21}As$ quantum well. The dashed line marks the onset of the continuum; the well barrier depth is $-V_0=-95.65$ meV.

stress which makes HH1 and LH1 coincide at $\mathbf{k}_{\parallel}=\mathbf{0}$.

Figure 5 shows the subbands in the $\langle 10 \rangle$ direction of a quantum well of width 78 Å, without an externally applied stress. The dashed line denotes the onset of the continuum, where χ_l and χ_h become pure imaginary. We note that HH3 band at high $\mathbf{k}_{\parallel}$ has an energy below the well depth $-V_0=-95.65$ meV, these confined states are resonant with the continuum, the extra energy coming from the motion parallel to the interfaces. These states are stationary in our model: they become Fano resonances which decay into the states of the continuum when some other interaction, like phonon or impurity scattering, changes the value of $\mathbf{k}_{\parallel}$.

A different kind of behavior arises from the LH2 band, which starts as a confined level for small $\mathbf{k}_{\parallel}$, then it meets the continuum line, where it ceases to exist as a discrete level. As the value of $\mathbf{k}_{\parallel}$ increases, instead of a real bound state one obtains a virtual antibound state with a diverging wave function at infinity. When the well width (or more precisely the parameter V_0L^2) decreases, the whole LH2 band moves towards the continuum until eventually it disappears. When this happens, a new transmission peak in the continuum below $-V_0$ occurs as in the one-dimensional scattering problem. Uniaxial stress can be used in order to tune the energy of these transmission peaks.

We emphasize that discrete states, resonances, and continuum states can all be determined in a natural way by our method. Clearly, the four-component envelope-function approximation becomes less accurate for excited states, when the energy differences become comparable to the spin-orbit splitting, which for GaAs is $\Delta=340$ meV. For a more accurate treatment the procedure must be extended to include the $\mathbf{k}\cdot\mathbf{p}$ coupling to the split-off band.

V. CONCLUSIONS

We have studied hole subbands of GaAs-$Ga_{1-x}Al_xAs$ quantum wells under uniaxial stress. Within the effective-mass approximation, energy levels and envelope functions can be determined exactly by solving the effective-mass equation in each bulk material. Use of reflection symmetry allows us to decouple the spin-degenerate subbands, and to obtain the energy eigenvalues as the zeros of an 8×8 determinant. Uniaxial stress can enhance the mixing between different valence subbands at $\mathbf{k}_{\parallel}\neq\mathbf{0}$, and the mixing can be analyzed using the form of the wave functions. Resonant states of the Fano type have been shown to arise.

Our method yields a simple and unified treatment of confined states, resonances, and continuum levels. The extension to superlattices is straightforward, but since the superlattice wave number k_s is not parity invariant, the full 16×16 determinant must be used in that case. The exact wave functions may be useful in studying tunneling between two distant quantum wells, as well as resonance scattering at an energy below the well depth; they can also be the starting point for the construction of exciton or impurity levels, with the main advantage that the dependence of the envelope function on z is analytically known.

ACKNOWLEDGMENTS

We thank Professor M. Altarelli for allowing us to compare our results with his variational wave functions, as well as for his interest in our work. We gratefully acknowledge useful discussions with Professor A. Baldereschi. This work was supported in part by the Italian Research Council [Consiglio Nazionale delle Ricerche (CNR)].

[1]S. R. White and L. J. Sham, Phys. Rev. Lett. **47**, 879 (1981).

[2]G. Bastard, Phys. Rev. B **24**, 5693 (1981); **25**, 7584 (1982).

[3]A. Fasolino and M. Altarelli, in *Two-Dimensional Systems, Heterostructures and Superlattices,* edited by G. Bauer, F. Kuchar, and H. Heinrich (Springer-Verlag, Berlin, 1984), p. 176; M. Altarelli, J. Lumin. **30**, 472 (1985).

[4]M. Altarelli, in *Heterojunctions and Semiconductor Superlattices,* edited by G. Allan, G. Bastard, N. Boccora, and M. Voos (Springer, Berlin, 1986); see also the review article G. Bastard and J. A. Brum, IEEE J. Quant. Electronics **QE-22**, 1625 (1986).

[5]G. D. Sanders and Y. C. Chang, Phys. Rev. B **31**, 6892 (1985).

[6]J. N. Schulman and Y. C. Chang, Phys. Rev. B **31**, 2056 (1985); **33**, 2594 (1986); Y. C. Chang and J. N. Schulman, *ibid.* **31**, 2069 (1985).

[7]M. Jaros, K. B. Wong, and M. A. Gell, Phys. Rev. B **31**, 1205 (1985); D. Ninno, M. A. Gell, and M. Jaros, J. Phys. C **19**, 3845 (1986).

[8]G. E. W. Bauer and T. Ando, Phys. Rev. B **34**, 1300 (1986).

[9]G. D. Sanders and Y. C. Chang, Phys. Rev. B **32**, 4282 (1985).

[10]A. Pinczuk, H. L. Störmer, R. Dingle, J. M. Worlock, W. Wiegmann, and A. C. Gossard, Solid State Commun. **32**, 1001 (1979).

[11]R. Sooryakumar, D. S. Chemla, A. Pinczuk, A. C. Gossard, W. Wiegmann, and L. J. Sham, Solid State Commun. **54**, 859 (1985).

[12]G. D. Sanders and Y. C. Chang, Phys. Rev. B **32**, 5517 (1985).

[13]J. M. Luttinger and W. Kohn, Phys. Rev. **97**, 869 (1955).

[14]G. L. Bir and G. E. Pikus, *Symmetry and Strain-Induced Effects in Semiconductors* (Wiley, New York, 1974).

[15]K. Suzuki and J. C. Hensel, Phys. Rev. B **9**, 4184 (1974).

[16]See Ref. 4 for a detailed discussion of boundary conditions.

[17]This conclusion holds independently of the phase chosen for σ, due to the fact that the matrices representing T and σ in (13) and (14) always anticommute. However, relation (15) between the operators holds only because of our particular choice of taking σ real.

[18]Variational wave functions with this property have been used in Ref. 5.

[19]S. S. Nedorezov, Fiz. Tverd. Tela **12**, 2269 (1970) [Sov. Phys. Solid State **12**, 1814 (1971)].

[20]*Landolt-Börstein Numerical Data and Functional Relationships in Science and Technology,* edited by O. Madelung

(Springer, Berlin, 1982), Group III, Band 17.
[21]A. Onton, in *Festkörperprobleme XIII,* edited by H. J. Queisser (Vieweg, Braunschweig, 1973), p. 59.
[22]R. C. Miller, A. C. Gossard, D. A. Kleinman, and O. Munteanu, Phys. Rev. B **29**, 3740 (1984).
[23]S. Adachi, J. Appl. Phys. **58**, R1 (1985).
[24]M. Altarelli (private communication).